

Effects of Surface Tension on the Dislocation Structures of Diblock Copolymers

Y. Liu, M. H. Rafailovich,* and J. Sokolov*

Department of Materials Science and Engineering, SUNY at Stony Brook,
Stony Brook, New York 11794-2275

S. A. Schwarz

Physics Department, Queens College, Flushing, New York 11367

S. Bahal

Exxon Research and Engineering Company, Annandale, New Jersey 08801

Received May 8, 1995; Revised Manuscript Received October 25, 1995[®]

ABSTRACT: Cross-sectional and plane view TEM, in conjunction with atomic force microscopy (AFM), was used to study the dislocations produced within PS–PVP diblock copolymer films. The results showed that islands or holes on the surface of multilayer films were produced by prismatic loop dislocations with a screw component in the layers below the surface. Only the contours at the vacuum surface obtained by AFM could be fit with classical elasticity theory. Flattening of the surface by the surface tension when the films were ordered on a silicon substrate induced a large amount of compression in the lamella beneath the surface. In films less than 3/2 lamellar layers thick, this compression is shown to induce a transition from lamellar to perpendicular cylinders at the edge of the island or holes. This transition was suppressed when the diblock copolymer molecular weight was decreased or when the films were ordered at a low surface tension interface. A qualitative model which estimates the degree of chain stretching induced by the surface tension is proposed to explain these effects.

1. Introduction

Ordering in polymers induced by the presence of a surface has been of considerable interest both theoretically and experimentally. Immiscible binary homopolymer blends form a phase-separated mixture with each component segregating to its lower surface tension interface.¹ Symmetric diblock copolymer films in contact with a solid surface form a lamellar mesophase oriented parallel to the surface when the difference between the surface tensions of the two blocks is sufficiently high so that the block with lower surface tension segregates to the vacuum interface, while the other segregates to the substrate.^{2,3} The thickness of the film, t_n , is quantized according to L , the thickness of one lamellar period, as $t_n = (n + 1/2)L$, where n is the number of layers. However, if the film is prepared in a disordered state with an initial thickness $t \neq t_n$, elevated or depressed domains of height L (islands or holes) form at the free surface.^{4,5} Maaloum et al.⁶ have studied the edge profiles of the surface domains using atomic force microscopy (AFM). Based upon the hypothesis that the surface distortion was induced by a single edge dislocation under the monolayer layer directly below the surface, the shape of the free surface was fit with a model developed by Pershan⁷ and Kleman⁸ for the analogous situation in a semiinfinite smectic-A liquid crystal. In order to obtain good agreement for the measured profile, a smectic penetration length, κ ($\kappa = (K/B)^{1/2}$, where K is the splay modulus and B is the compressional modulus), 20 times smaller than the mean field estimate had to be used.⁶ The discrepancy between theory and experiment was attributed to the omission of the surface tension, which is the dominant term in the free energy at the vacuum surface, and lack of precise knowledge on the position of the edge dislocation within the sample.

These two problems were addressed by Turner et al.,⁹ who adapted continuum classical elasticity theory specifically for the case of symmetric diblock copolymers. The effect of the surface energy term, as will be shown later, is to minimize the gradient of the surface deformation and determine the position of the edge dislocation. Fitting the AFM data of Maaloum et al.⁹ with this model, they found $K = 10^{-6}$ dyn and $B = 10^6$ dyn/cm². From these values, they obtained the interfacial tension between the copolymer blocks as $\gamma_{AB} = (KB)^{1/2} = 0.9$ dyn/cm, which is comparable to the values obtained by Russell and co-workers for polystyrene–poly(methyl methacrylate) (PS-*b*-PMMA) block copolymers.¹⁰

These previous studies focused mainly on the surface morphology and the profiles of surface contours. However, the nature of the dislocation which induces the surface distortion and the propagation of the deformation through the lamellar film have not been investigated systematically. In fact, it was recently shown by Carvalho and Thomas¹¹ that even when the lamellae were not oriented parallel to the surface, islands or holes with the same surface contours can result.

In this paper, we report a systematic study, using ultramicrotomy, transmission electron microscopy (TEM), and atomic force microscopy (AFM), of the nature of the dislocation and the corresponding distortion of the lamellar layers which results in a surface island or hole morphology. The system chosen is that of symmetric poly(styrene-*d*₈-*b*-2-vinylpyridine) (PS–PVP) diblock copolymers, which have been shown to produce highly ordered films on silicon substrates.¹² The surface topography was characterized by AFM, and the induced dislocations beneath the surface were measured by cross-sectional and plane view TEM. The data were used to test the theoretical calculations of Turner and co-workers.⁹ The results show that the continuum model breaks down almost immediately below the

[®] Abstract published in *Advance ACS Abstracts*, December 15, 1995.

Table 1. Characteristics of the Block Copolymers and Homopolymers Used in This Study

	composition	polymerization index	f_{PVP}
diblock copolymer	PVP-PS	200-200	0.5
	PVP-PS	510-540	0.49
	PVP-PS	800-870	0.48
homopolymer	PVP	3000	1.0
	PS	6700	0

vacuum surface due to the rapid change in the profile from the large compression of the film by the surface tension. The difference in the structure of the dislocation in the presence of large and small interfacial tension is explained in terms of the stretching energy of the block copolymer chains required to maintain constant density within the sample. The effect of chain length on the configurations of the diblock copolymers generating the defects that result in the island or hole morphology is investigated. The free energies corresponding to the defect structures are estimated in order to interpret the experimental data and explain the observed dependence of structure on molecular weight. A transition from cylindrical structure ordered perpendicular to the surface to the edge dislocation in parallel lamellae is observed as the molecular weight of the PS-PVP diblock copolymer is decreased.

2. Experimental Section

Symmetric monodisperse diblock copolymers of poly(styrene-*d*₈-*b*-2-vinylpyridine) (PS-PVP) and poly(2-vinylpyridine) (PVP) homopolymer were synthesized via anionic polymerization and characterized by ¹³C NMR and mass microanalysis to determine the PVP volume fraction.^{13,14} The polymerization indices are summarized in Table 1. The interaction parameter, χ , for PS-PVP diblock copolymer was previously measured to be $\zeta = -0.033 + 63/T$.¹³ For the annealing temperature, $T \approx 180$ °C, used in our study, $\chi = 0.1$, which is well above the χ at the order-disorder transition temperature for all the block copolymers used in this study.

Polymer films ordered on the "hard" surface were prepared by spin-casting the block copolymers from toluene solution directly onto native oxide covered silicon wafers with a surface roughness of 6 Å. Samples on the "soft" surface were prepared by first spin-coating a layer approximately 5000 Å thick of monodisperse PVP onto the polyimide substrate. The PVP molecular weight, $M_w = 300\,000$, was much larger than that of the PVP block so as to minimize the penetration of PVP homopolymer into the lamellae. The PVP films were annealed at 180 °C in vacuum (10^{-4} Torr) for 2 h to relax any distortions induced by the spinning process. The block copolymer films were spun cast onto glass slides and floated from water onto the PVP-covered polyimide substrate. All the samples were annealed again in vacuum at 180 °C for 4 days and quenched at room temperature. The surface topography was measured using a Digital Nanoscope III AFM with a Si₃N₄ tip and a force of ≤ 20 nN in the contact mode.

For plane view TEM microscopy, the films were floated from the silicon wafers onto Cu mesh grids. KOH solution at ~ 90 °C was used to dissolve the silicon oxide and release the films which are bonded via the PVP blocks to the silicon surface.

To obtain cross-sectional views of ordered films, the annealed samples were floated from KOH solution onto polyimide substrates coated with 5000 Å of PVP homopolymer ($M_w = 300\,000$) to minimize interfacial strain during microtoming. To protect the surface, the samples were coated with a 2 μm thick layer of PS ($M_w = 670\,000$). The samples were then annealed at 120 °C for 5 min to enhance the mechanical strength at the upper and lower interfaces between the diblock copolymer films and the hPS and PVP homopolymer layers. Approximately 800 Å thick sections were cut by ultramicrotomy using a diamond knife at room temperature. In order to minimize the deformation from the knife, the cutting

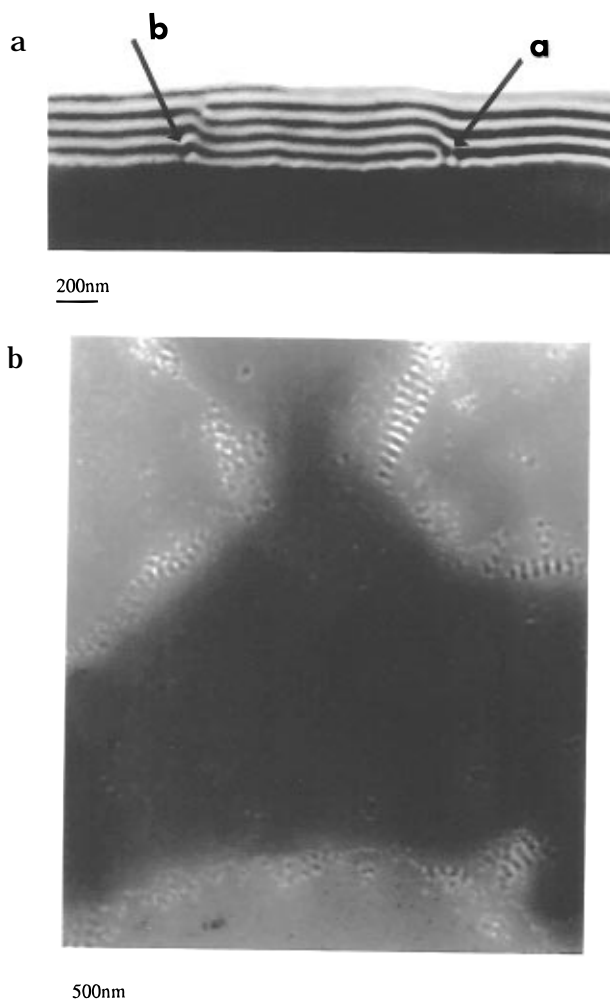


Figure 1. (a) Cross-sectional TEM micrograph of the 870-800 dPS-PVP diblock copolymer film ordered on a silicon surface. (b) TEM plane view of the surface for the same copolymer film shown in (a).

direction was chosen parallel to the lamellar orientation. The sections floated on water were collected on copper mesh grids. All TEM samples were stained in iodine vapor for 12 h. The iodine reacts preferentially with PVP, rendering the PVP microdomains dark in the image of the electron beam. The stained sections were then observed with a Philips/CM-12 TEM operated at 120 kV, using a side entry goniometer stage.

3. Defects in Multilayer Symmetric Diblock Copolymer Films

Figure 1a is a cross-sectional TEM micrograph of an ordered dPS-PVP diblock copolymer film of polymerization indices 870-800 approximately 3000 Å thick, originally spin-coated on a silicon substrate. It should be emphasized that the morphology of the dislocations and the associated deformation of the lamellar layers are unaffected by the sample preparation and the cutting techniques described in the Experimental Section. From the figure we see what appears to be two edge dislocations which delineate the boundaries under an island at the free surface: a +1 edge dislocation under the first layer below the upper surface, and a -1 edge dislocation located diagonally 1/2 lamellar layer above the silicon substrate. Figure 1b is the plane view of the sample shown in Figure 1a showing that the film surface has an interconnected island morphology. In approximately 30 cross-sectional views of films, 4-6 lamellar layers thick, with similar surface island or hole

structures, we found that the +1 and -1 dislocation couples were correlated and always occurred in different lamellar layers. The number of lamellar layers separating the dislocations varied randomly for each defect. We therefore can infer that a prismatic loop dislocation with a screw component seems to be the preferred method for generating islands or holes on the surface of multilayered films. Future experiments are planned to obtain a serial set of cross-sections from one island which should provide a three-dimensional view and identify the nature of the dislocation more precisely.

It has been argued in several models^{8,9} that the surface tension, γ , and the interfacial tension, γ_{AB} , should determine the equilibrium position of the defect. If $\gamma < \gamma_{AB}$, the dislocation should be located at the solid surface, while if $\gamma > \gamma_{AB}$, the dislocation is driven to the center of the lamellae. In our case, $\gamma \gg \gamma_{AB}$, and this prediction clearly does not fit the observed pictures. This has been shown by Muthukumar¹⁵ to be related to the dynamics of the defect formation. The process occurs in two stages.¹⁵ In the first stage, the copolymer chains segregate from the disordered state into lamellar microdomains. The dislocations arise arbitrarily in the film as the microdomains align themselves relative to the sample surface. In the second stage, the dislocations formed in stage I coalesce to obtain the global energy minimum for the whole film. This stage requires the coordinated motion of many chains, and the dynamics can be much slower than those involved in stage I. It is possible that stage II may be out of our experimental time range, and hence the defects may not be at their equilibrium position. In previous experiments,¹⁶ we observed that the number and size of the islands as well as the internal ordering of the film changed rapidly within the first 48 hours of annealing. This could be tentatively identified as stage I. No further changes were observed upon subsequent anneals up to 14 days. From Figure 1a, we can see that once the chains are well oriented into lamellae parallel to the surface, any further motion of the islands across the surface clearly cannot occur just by diffusion across the uppermost lamella. Rather, in order for the islands to grow by consolidation, the defects must coalesce. This motion is apparently quite complicated in multilayer films and can be slower than our observation time.

It is also interesting to notice that the extra half plane of the dislocation is always observed in the PVP phase. The PVP layer behaves as if it were stiffer than the dPS layer, i.e., it tends to form the dislocation core, while the dPS layer is forced to bend around it. This result is somewhat surprising since PVP and PS homopolymer melts have been shown to have similar entanglement lengths and viscosities.¹⁷

The profiles of the curved interfaces associated with the -1 dislocation are digitized and plotted in Figure 2. The values at the right side of the dislocation are the gradients, $du(x)/dx$, for each dPS-PVP interface at $x = 0$, or the position where $u(x)$ reaches half of its maximum value. It should be pointed out that the very first dPS layer adjacent to the vacuum surface cannot be seen clearly in Figure 1a since dPS does not stain in iodine vapor and has no contrast with the polystyrene overlayer. The position of this layer can only be determined from the fine crack observed from incomplete fusion between the film surface and the thick PS overlayer (open circles). The composition of this dPS surface layer was confirmed by secondary ion mass spectrometry and the neutron reflectivity spectra of the

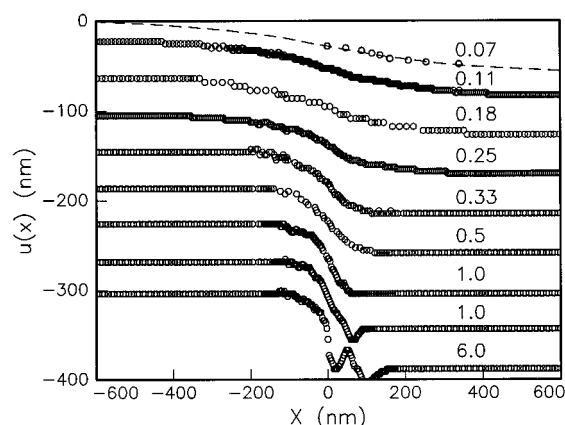


Figure 2. Profiles of the contours at the free surface and the interfaces above the -1 dislocation shown in Figure 1a. The numbers on the right correspond to $du(x)/dx$ at $x = 0$. The dashed line is the AFM profile. The edge of the PS cover layer in the TEM image is designated by (○).

Table 2. Parameters Used To Fit the Profiles at the Free Surface and the dPS-PVP Interface Immediately below the Surface above the -1 Edge Dislocation Shown in Figure 1a

interface	ΔH (nm)	H_u (nm)	H_d (nm)	Γ_u	κ (nm)
air/PS (AFM)	32	320	70	25	10
PS/PVP (TEM)	32 ^a	300 ^a	67 ^a	25	5

^a Determined from the TEM micrograph in Figure 1a.

ordered dPS-PVP block copolymer film.^{12,16} The topography of the layer was determined with AFM and is shown as a dashed line in Figure 2.

The profile of the surface contour of an island, as measured by AFM, was first used to test the model of Turner et al. in a manner similar to that described in ref 9. In the continuum limit, the free energy for the lamellar film with surface tension γ is given by⁹

$$f(x,y) = \frac{B}{2} \left(\frac{\partial u}{\partial z} \right)^2 + \frac{K}{2} \left(\frac{\partial^2 u}{\partial x^2} \right)^2 + \frac{\gamma}{2} \left(\frac{\partial u_h}{\partial x} \right)^2 \quad (1)$$

where u is the vertical displacement of a lamellar layer from its equilibrium position and u_h is the displacement variable at the surface. Only the second-order terms are included in the free energy expansion since it is assumed that $du(x)/dx$ is small or u varies slowly in the continuum limit.

Minimizing the free energy given in eq 1 and simplifying the calculation using Fourier transform, the displacement at the free surface for the lamellar copolymer film ordered on a solid substrate is given by⁹

$$u(x, \Gamma_u, K) = \frac{\Delta h}{2\pi} \int_0^\infty \frac{\sin(qx)}{q} \frac{(e^{2\kappa h_d} q^2 + 1)(1 + G_u)e^{2\kappa h_u q^2}}{G_u e^{2\kappa(h_d+h_u)q^2} + 1} dq \quad (2)$$

Here, Δh is the discontinuity across the dislocation, h_d and h_u are the distances from the center of the dislocation line to the lower and upper surface, respectively, and Γ_u is defined as the dimensionless surface tension at the upper surface of the film (i.e., $\Gamma_u = \gamma_{up}/(KB)^{1/2}$, and $G_u = (1 + \Gamma_u)/(1 - \Gamma_u)$). For the solid substrate, the dimensionless surface tension at the lower surface of the film, $\Gamma_d = \gamma_d/(KB)^{1/2} \rightarrow \infty$. In Table 2, we list the values of all parameters used for fitting the upper surface contour, where $h_u + h_d$ is fixed as the total

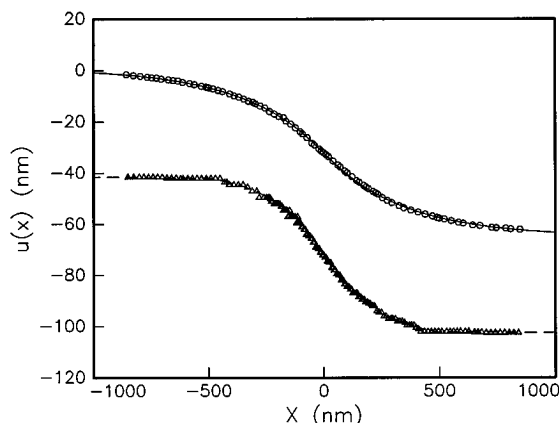


Figure 3. Profiles of the distortion induced by the -1 edge dislocation in Figure 1a at the free surface (○) and the first dPS/PVP interface (△) beneath the free surface. The solid line and the dashed line are the best fits to the model of Turner and co-workers in ref 9 for the upper and lower data curves, respectively.

thickness of the film. The data are plotted as open circles in Figure 3, and the best χ square fit is shown as a solid line. From the fit value of Γ_u and κ and substituting $\gamma_{PS} = 29$ dyn/cm at 180°C ,¹⁸ we calculate for the compressional and splay moduli $B \approx 1 \times 10^6$ dyn/cm² and $K \approx 1 \times 10^{-6}$ dyn, respectively. The value of B is close to $B_0 = 3 \times 10^6$ dyn/cm², the compressive modulus of bulk polystyrene.¹⁹ As far as we know, no independent measurement of K for any block copolymer has been reported in the literature. The square root of the quantity, $(KB)^{1/2} \approx \gamma_{\text{dPS-PVP}} \approx 1.2$ dyn/cm for dPS-PVP diblock copolymer, is slightly higher than but roughly the same order of magnitude as that reported in the previous experiments for PS-PMMA diblock copolymers.¹⁰ This is consistent with the larger value of χ (0.1 for PS-PVP and 0.04 for PS-PMMA) for the PS and PVP block copolymers and the scaling of γ_{AB} with $\chi^{1/2}$.

The same fitting procedure using eq 2 was also applied to the dPS-PVP interface immediately below the free surface. The profile obtained from the cross-sectional TEM micrograph in Figure 1a is shown as open triangles in Figure 3, and the dashed line is the best χ square fit to the data. In this case only, Γ_u and κ were varied while Δh , h_d , and h_u were fixed to the values measured from the TEM micrograph. The values of the fitting parameters are also listed in Table 2. From the table, we can see that the value of κ , which is a dominant factor in determining the gradient of the deformed interface, decreases by a factor of 2 in the layer below the surface. This difference between the two fit values of κ is not reasonable since in the continuum model K and B are intrinsic properties of the material and should remain constant throughout the layers. Hence eq 2 breaks down almost immediately in the interior of the sample.

The reasons for this become apparent from a careful examination of Figure 2 and eq 1. At the vacuum surface, the term proportional to γ dominates the free energy expression. For the layers below the surface, the tension is given by γ_{AB} and the solution to the differential equation (eq 2) becomes more sensitive to the other terms. In eq 1, it is assumed that du/dx is a slowly varying function of x . This is only true if the deformation within a given layer is negligible. From the figure, it can be seen that in fact the gradient is very large immediately above the dislocation and decreases rapidly

as the free surface is approached. The rate of decrease is much larger than for a normal smectic-A liquid crystal, where the curvature of the distortion remains constant for many layers.⁷ In addition, in the continuum limit, chain stretching is assumed to be uniform and given by the moduli, K and B , which are assumed constant throughout the film. The energy associated with variable deformation of individual polymer chains is not included in eq 1. The two interfaces shown in Figure 3 correspond to the free end and the dPS/PVP junction points of the same chains. The two different slopes can only be obtained by compressing the polymer chains, and the degree of compression is different for each layer.

From Figure 2, it can be seen that the compression due to the large surface tension at the free surface (29 dyn/cm for dPS) acts by severely compressing the dPS chains in order to minimize the total surface area. This is illustrated at the $+1$ dislocation in Figure 1a, which is located one L beneath the surface. The asymmetry of the gradient at the interfaces above and below the $+1$ dislocation results from the large difference in surface tension acting at the upper and lower interfaces of the dislocation. Therefore, the exact shape of the interface in any particular layer below the surface, even if it is far from the actual dislocation, cannot be determined only from eqs 1 and 2. Additional terms must be included which model the energy lost in locally compressing the copolymer chains to flatten the surface dislocation and the enthalpy gained in ordering the block copolymers in nonintegral layers parallel to the surface. In fact, it has been previously shown by Liu et al.¹⁶ that when the enthalpy term is decreased by reducing the PVP block size in very asymmetric PS-PVP diblock copolymers ($f < 0.28$), the surface-induced order is poor and islands do not form in films thicker than approximately 3 layers.

4. Defects in Very Thin Films

4.1 Effect of Surface Tension on the Configurations of Copolymer Chains at Defects. In the previous section, we showed that islands or holes on the surface of symmetric diblock copolymer films are induced by prismatic loop dislocations with screw components in the lamellae if the film consists of more than two lamellar layers. The effect of the surface tension on the dislocation core was shown to be partially shielded by the copolymer layers above the dislocation. In this section, we discuss the effects of confining the defect between the vacuum and solid interfaces when the film thickness, t , is less than $2L$.

Figure 4a is a TEM plane view of an 870–800 dPS-PVP copolymer film with initial thickness $t = 839$ Å ($1/2L < t < 3/2L$) ordered on the silicon substrate. Figure 4a shows a large light circular region in the middle of the micrograph, which indicates the film is thinner there than in the surrounding region, which appears dark. It has been reported previously^{12,16} that PVP interacts strongly with silicon, and the block copolymer always completely wets the silicon substrate even if $t \leq 1/2L$. When the initial film thickness is in the range $1/2L < t < 3/2L$, the extra material forms an incomplete second lamellar layer, which appears as a hole at the free surface. AFM and dynamic secondary ion mass spectrometry (dSIMS) profiling of the film surface confirm that the light region in Figure 4a corresponds to the $1/2L$ layer of dPS-PVP adsorbed to the silicon substrate, and the dark region corresponds to the second

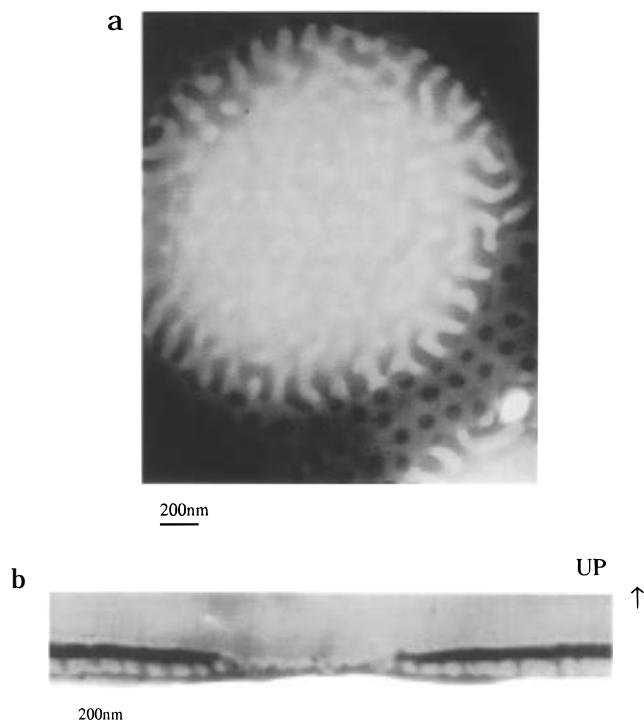


Figure 4. (a) TEM plane view of a hole at the surface of an ordered 870–800 dPS–PVP diblock copolymer film with an initial thickness of 839 Å. (b) TEM cross-sectional view for the same copolymer film shown in (a).

homogeneously aligned lamella (dPS–PVP/PVP–dPS) parallel to the substrate. It is interesting to note in Figure 4a that the lamellae reorient from parallel to perpendicular to the substrate at the boundary of the hole. The reorientated lamellae appear to extend radially along the periphery of the hole, joining the upper and lower lamellar layers. The separation between the lamellae aligned perpendicular to the substrate is approximately 1400 Å, i.e., $\sim 2L$, or a factor of 2 greater than the confinement of the lamellae ordered parallel to the substrate. A series of dark spherical spots with a diameter of approximately 700 Å which are aligned in a two-dimensional hexagonal lattice are also observed along the periphery of the hole. The decreased contrast between the dark spots and the background in Figure 4a indicates that these structures might lie beneath a uniform surface lamellar layer.

Figure 4b is the cross-sectional TEM micrograph of the same copolymer film shown in Figure 4a. From the micrograph, we see that there is a uniform lamellar layer at the silicon substrate and at the vacuum interface. The region between the two parallel lamellar layers is spanned by short cylindrical domains, approximately $L/2$ in height. These domains correspond to the dark circular structures observed in the plane view micrograph. It is interesting to note that these structures become progressively more elongated in the direction parallel to the surface as they merge back into the lamellar phase. This picture is qualitatively similar to the extended interface between a lamellar and a cylindrical phase shown by Turner et al. in ref 20.

The transition from lamellar ordering in a symmetric diblock copolymer film to perpendicular orientation with respect to the substrate has been previously reported by Russell and co-workers²¹ when the copolymer was confined between two parallel plates and by Carvalho et al.¹¹ at the step of a terraced diblock copolymer droplet. The air interface is analogous to the parallel

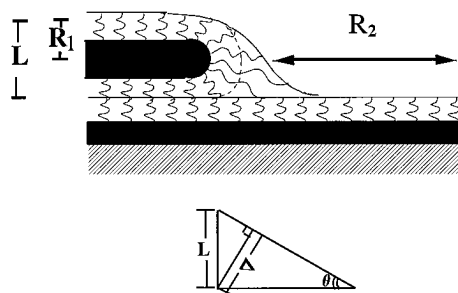


Figure 5. Schematic of an edge dislocation along the boundary of a hole at the surface of a diblock copolymer film.

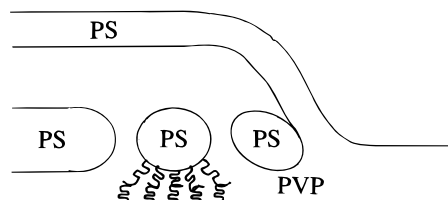


Figure 6. Schematic of cylindrical structures along the boundary of a hole at the surface of a diblock copolymer film.

plate geometry as is evidenced by the relatively flat profile obtained for the large value $\gamma/(KB)^{1/2} \sim 25$ in eqs 1 and 2. This situation for a two-layer film is illustrated in Figure 5, which was drawn by removing the middle layers in Figure 1a and superimposing the AFM surface profile above the -1 dislocation nearest the silicon substrate. From the figure, it can be seen that in order for the PS chains which originate at the PVP interface to reach the vacuum surface, a significant amount of stretching must occur. The maximum excess energy per chain can then be estimated (in units of $a = 1$ and $kT = 1$) as

$$\Delta f_{\text{stretch}} = \frac{(L + \Delta)^2}{2N} - \frac{L^2}{2N} \approx \frac{(2\alpha + \alpha^2)}{2} \frac{L^2}{N} \quad (3)$$

where α is obtained from the slope of the surface contour by $\Delta = \alpha L$ (Figure 5). The difference in energy per chain between the bulk lamellar and cylindrical phases is given to first order by

$$\Delta f_{\text{cyl-lam}} \approx \frac{\gamma_{AB}}{N} \times \text{const} \quad (4)$$

where the constant is of unit order.²⁰ $\Delta f_{\text{stretch}}$ can therefore become much larger than $\Delta f_{\text{cyl-lam}}$, thereby inducing the transition observed in Figure 4a.

Disorientation of the lamellar ordering can also be observed to a lesser degree in the multilayer films as well. This is shown in Figure 1b, which is a plane view of the film shown in cross-section in Figure 1a. In thick films, the stress can be relieved among the layers and the amount of disorientation is smaller. This can be seen in Figure 1a, where the defect labeled "a" at the silicon interface is due to the abrupt flattening of the dislocation profile propagating from the -1 defect near the vacuum surface. The spherical defect labeled "b" which occurs in the two layers adjacent to the silicon surface results from the large gradient at the position of the $+1$ dislocation. This defect gives rise to the small cylindrical regions observed in Figure 1b.

From these two views of the film, we can conclude that some dislocation will occur in any film which is highly ordered parallel to a hard surface. The constraint of $\gamma \rightarrow \infty$ will produce a small region of disloca-

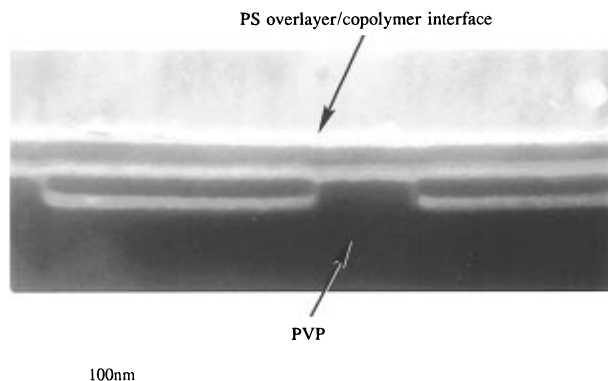


Figure 7. Cross-sectional TEM micrograph of the 870–800 dPS–PVP diblock copolymer film with an initial thickness of 839 Å ordered on the surface of a 5000 Å thick PVP ($M_w = 300\,000$) layer spin-coated on a polyimide substrate.

tion when the defect propagates to the flat surface. The magnitude or nature of the dislocation will be a function of the distance between the dislocation and the hard surface. For most of the samples studied, this position was arbitrary and was not a quantized function of the sample thickness. From the plane view, it is difficult to determine the position or the nature of the dislocation within the sample.²² One can only measure the planar extent of the dislocation region. Therefore, for a given molecular weight of PS–PVP diblock copolymer, there is no critical layer thickness for which the disorientation observed at the defects in the plane view will disappear. From Figure 2, we can only conclude that the lamellar configuration for the 800–870 dPS–PVP diblock copolymer becomes stable when the slope of the contour satisfies the condition $(du(x)/dx)_{x=0} \leq 1$. This corresponds to a maximum stretching that the chains can undergo and still retain their lamellar configuration of approximately 40%.

When one of the confining surfaces is removed, the compression at the PS interface disappears and $\Delta F_{\text{stretch}} \rightarrow 0$. The islands can now form by inducing a pure edge dislocation in the lamellar structure with a gradient corresponding to $\theta \approx 90^\circ$ and $\alpha = 0$. This is illustrated in Figure 7, which shows a cross-sectional TEM micrograph prepared by annealing a layer of the 800–870 dPS–PVP diblock copolymer on a thick PVP substrate. In this case, the interfacial tension at the PVP interface is much lower than that at the vacuum surface ($\gamma_{AB}/\gamma \sim 1 \times 10^{-3}$). Perfect islands are seen to form only in the PVP homopolymer layer, while AFM microscopy shows that the vacuum surface is completely flat.²³

This effect is also observed to a lesser extent in multilayer films. Figure 8 is a TEM micrograph of a multilayer film originally ordered on a silicon substrate and then transferred onto a thick PVP substrate and annealed for 2 h at 180 °C. Even though the annealing time is relatively short, we see that the islands are already relaxing into the PVP homopolymer layer and that the compression of the lamellae is greatly decreased.

4.2 Effect of Molecular Weight on the Configurations of Copolymer Chains at Defects. PS–PVP diblock copolymers of two other polymerization indices, 200–200 and 540–510, were used to study the molecular weight dependence of the disorientation near the island or hole boundaries. Figures 9 and 10 are the TEM plane view micrographs of the 540–510 and 200–200 PS–PVP diblock copolymer films originally ordered

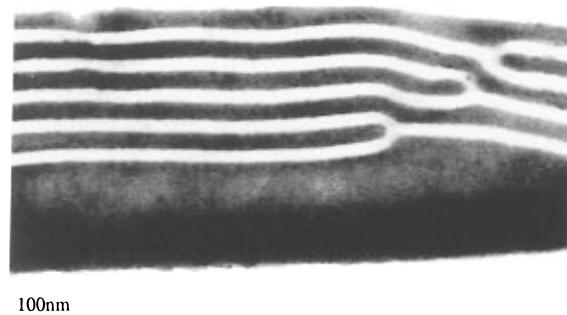


Figure 8. Cross-sectional TEM micrograph of a 3000 Å thick 870–800 dPS–PVP copolymer film originally ordered on a silicon substrate and then transferred onto a 5000 Å thick PVP substrate and annealed at 180 °C for 2 h.

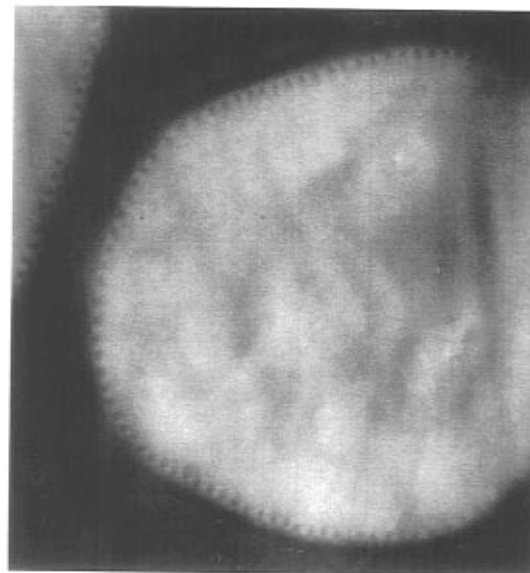


Figure 9. TEM plane view of a hole at the surface of an ordered 540–510 diblock copolymer film of initial thickness 540 Å.

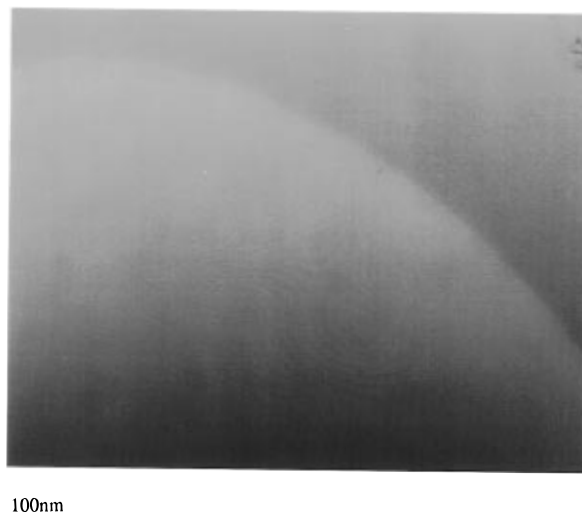


Figure 10. TEM plane view of a hole at the surface of an ordered 200–200 diblock copolymer film of initial thickness 450 Å.

on the silicon surfaces, with thicknesses ranging from $1/2L$ to $3/2L$. These figures show that reorientation of lamellae occurs only for the 540–510 diblock copolymer

film. The morphology observed in Figure 9 is similar to that observed on the 870–800 dPS–PVP diblock copolymer shown in Figure 4a except that the disordered region is smaller and confined to the boundary of the hole. The periodic separation and the radial extension of the lamellae aligned perpendicular to the surface is ~ 550 Å, or $\sim L$. In contrast, for the 200–200 PS–PVP diblock copolymer film shown in Figure 10, we observe a clear-cut boundary of the hole without reorientation of lamellae. The uniform TEM contrast indicates that the holes are formed only via edge dislocations which, in this case, are stable near the vacuum interface. In order to try to understand the function of molecular weight in the transition from the reoriented lamellae to edge dislocations, we must examine more closely the free energy density associated with the parallel and perpendicular orientations.

Since the grafting density changes with molecular weight, let us now consider the total energy per unit area associated with the parallel and perpendicular configurations, F_{para} and F_{perpen} , respectively.

For the parallel orientation the energy associated with the edge dislocation is given by

$$F_{\text{para}} = F_{\text{stretch}} + F_{\text{PS/PVP}} \quad (5)$$

where $F_{\text{PS/PVP}}$ is the interfacial energy of the defect. F_{stretch} , the excess energy due to stretching the chains when the profile is flattened at a hard surface, is²⁴

$$F_{\text{stretch}} = \Delta f \Sigma$$

$$\Sigma = \Sigma^* \left[1 + H^2 - \frac{2}{15} K \right] \quad (6)$$

Σ is the interfacial area per chain for a curved interface, and $\Sigma^* \cong N^{1/3} \gamma_{\text{AB}}^{1/2} \cong N/L$ is the area per chain for a flat lamellar interface. $H = 1/2(1/R_1 + 1/R_2)$ and $K = 1/R_1 R_2$ are the mean and Gaussian curvatures, respectively for the two principal radii, R_1 and R_2 , at one point of curvature.²⁴ In our case, R_2 is the radius of the hole or island, $R_1 \sim L/2$ (Figure 5), and to first order $\Sigma \sim \Sigma^*$. F_{para} per unit area can then be written as

$$F_{\text{para}} \cong \left(\frac{2\alpha + \alpha^2}{2} \right) + \frac{\pi}{4} \gamma_{\text{AB}} \quad (7)$$

where we have substituted $F_{\text{stretch}} = \Delta f_{\text{stretch}} \Sigma$ and approximated the edge dislocation as a semicylindrical surface.

For the perpendicular cylinder configuration at the edge of the defect shown in Figure 4, the free energy per unit area is

$$F_{\text{perpen}} = F_{\text{cyl-lam}} + F_{\text{interface}} \quad (8)$$

$F_{\text{interface}}$ is the additional energy term imposed by the constant-density constraint at the interface between the lamellar and cylindrical structures. In the case of the PS–PVP diblock copolymer, the large difference in surface tension between the PS and PVP blocks requires that only one component be present at each interface. This forces a lamellar structure at both the Si and vacuum interface regardless of the bulk structure.¹⁶ When the total film thickness $t < 3/2L$, the interfacial region is confined to one layer and the interfacial structure must change more rapidly than can be calculated with the continuum model described by Turner et al.²⁰

A more realistic approach is described by Olmsted and Milner,²⁵ who were able to predict the optimum curvature of a given phase by minimizing the chain stretching at the unit cell boundaries. Clearly, this factor must also play a role in the structure assumed by the cylinders and probably accounts for the differences in the configurations observed between the 540–510 and 200–200 PS–PVP diblock copolymers. Unfortunately, the morphologies we observed are fairly complicated, and hence a detailed contour integral cannot be performed. We can only assume that significant chain stretching must occur to match the lamellar and cylindrical phases. Consequently, this term must be the predominant component of the interfacial energy and can be comparable to F_{stretch} for the parallel orientation. Whichever of the two configurations, lamellar plus edge dislocation or perpendicular cylinders, is assumed to make the island or hole in a confined film is determined by the difference in free energy ΔF between the two phases:

$$\Delta F = F_{\text{stretch}} - F_{\text{interface}} \quad (9)$$

where we have omitted the terms on each side that scale as L^{-1} . From Figure 6, one can see that as the molecular weight of the diblock decreases, the curvature of the cylindrical interface increases ($H \sim 1/L$). A critical L_c can then exist for which the stretching at the lamellar to cylindrical interface exceeds that imposed by γ on the simple edge dislocation near the vacuum surface in the parallel lamellar phase. In our case, we can see that as L decreases, the cylindrical–lamellar interface becomes more abrupt; i.e., the gradual elongation of the cylinders is not observed. We can argue that this too is consistent with Turner's model,²⁰ in which the size of the interfacial area is decreased as the interfacial energy increases. Finally, L_c is reached somewhere between $N = 1050$ and $N = 400$, where the cylindrical structures disappear completely.

5. Conclusion

We have observed that islands or holes on the free surface of multilayer PS–PVP diblock copolymer film ordered on flat silicon surfaces are induced by prismatic loop dislocations with screw components inside the copolymer film. The curvature of the associated distortion at PS/PVP interfaces in layers below the surface decreases as the distortion propagates away from the defect core to the free surface. Only the vacuum surface contour can be analyzed with classical elasticity theory since the leading surface tension is the dominant term in the free energy. In the layers beneath the surface, the deformation of the lamellae is large, i.e., comparable to the diblock copolymer chain dimensions, and hence the continuum limit is no longer applicable. It was shown that the maximum stretching sustained in the lamellar configuration by the 870–800 dPS–PVP diblock copolymer is approximately 40%. If the deformation imposed by the surface is large, cylindrical structures orientated perpendicular to the surface replace the edge dislocation in the vicinity of the islands. This lamellar to cylindrical transformation becomes less pronounced as the molecular weight of the diblock copolymer is decreased and finally disappears for the 200–200 PS–PVP diblock copolymer. A qualitative model based on the increase in the interfacial tension between the flat lamellar and cylindrical surfaces with increasing curvature of the cylinders was proposed. If the two-layer

diblock copolymer films are allowed to order on a low surface tension substrate, i.e., the surface of PVP homopolymer, perfect edge dislocations are formed in the PVP phase and no islands appear at the vacuum surface. This confirms the observation that the lamellar to cylindrical transformation occurs in order to minimize the local chain deformation induced by the confinement of the lamellae between two relatively hard interfaces.

Acknowledgment. We would like to thank A. H. King, O. Gebizlioglu, and . Olmsted for helpful discussions and M. S. Turner, E. Thomas, and E. J. Kramer for critically reading the manuscript. Support from NSF (DMR-9316157) and DOE (DE-FG02-93ER45481) is gratefully acknowledged.

References and Notes

- (1) Jones, R. A. L.; Kramer, E. J.; Rafailovich, M. H.; Sokolov, J.; Schwarz, S. A. *Phys. Rev. Lett.* **1989**, *62*, 280.
- (2) Coulon, G.; Russell, T. P.; Deline, V. R.; Green, P. F. *Macromolecules* **1989**, *22*, 2581.
- (3) Anastasiadis, S.; Russell, T. P.; Satija, S.; Majkrzak, C. F. *Phys. Rev. Lett.* **1989**, *62*, 1852.
- (4) Coulon, G.; Ausserré, D.; Russell, T. P. *J. Phys. Phys. (Paris)* **1990**, *51*, 777.
- (5) Coulon, G.; Collin, B.; Ausserré, D.; Chatenay, D.; Russell, T. P. *J. Phys. (Paris)* **1990**, *51*, 2801.
- (6) Maaloum, M.; Ausserré, D.; Chatenay, D.; Coulon, G. *Phys. Rev. Lett.* **1992**, *68*, 1575.
- (7) Pershan, P. S. *J. Appl. Phys.* **1974**, *45*, 1590.
- (8) Kleman, M. *Points, Lines and Surfaces*; Edition de Physique, Paris, 1978.
- (9) Turner, M. S.; Maaloum, M.; Ausserré, D.; Joanny, J.-F.; Kunz, M. *J. Phys. II Fr.* **1994**, *4*, 689.
- (10) Menelle, A.; Russell, T. P.; Anastasiadis, S. H.; Satija, S. K.; Majkrzak, C. F. *Phys. Rev. Lett.* **1992**, *68*, 67.
- (11) Carvalho, B. L.; Thomas, E. L. *Phys. Rev. Lett.* **1994**, *73*, 3321.
- (12) Liu, Y.; Rafailovich, M. H.; Sokolov, J.; Schwarz, S. A.; Zhong, X.; Eisenberg, A.; Kramer, E. J.; Sauer, B. B.; Satija, S. *Phys. Rev. Lett.* **1994**, *73*, 440.
- (13) O'Malley, J. J.; Crystal, R. C.; Erhardt, P. F. *Polym. Prepr. (Am. Chem. Soc., Div. Polym. Chem.)* **1969**, *10*, 796.
- (14) Dai, K. H.; Kramer, E. J. *Polymer* **1994**, *35*, 157.
- (15) Muthukumar, M. *J. Chem. Phys.* **1995**.
- (16) Liu, Y., et al. *Macromolecules* **1994**, *27*, 4000.
- (17) Shull, K. R.; Kellock, A. J. *J. Polym. Sci., Polym. Phys.*, in press.
- (18) Sauer, B. B., private communication.
- (19) Brandrup, J.; Immergut, E. H. *Polymer Handbook*, 3rd ed.; John Wiley and Sons: New York, 1989.
- (20) Turner, M. S.; Rubinstein, M.; Marques, C. M. *Macromolecules* **1994**, *27*, 4988.
- (21) Walton, D. G.; Kellogg, G. J.; Mayes, A. M.; Lambooy, P.; Russell, T. P. *Macromolecules* **1994**, *27*, 6225.
- (22) From Figures 4a, 4b, and 5, it can be seen that in our case the defects near the hole boundary are not pure Scherk's surfaces as suggested in ref 11.
- (23) This is strictly true only when the PVP layer thickness $t_{\text{PVP}} > L$. The height of the islands and the gradient of the contours were observed in previous experiments to decrease gradually as T_{PVP} was increased from 30 Å to L. Liu, Y. *BAPS*, vol 39, No. 1, 418.
- (24) Gido, P. S.; Thomas, E. L. *Macromolecules* **1994**, *27*, 849.
- (25) Olmsted, P.; Milner, S. *Phys. Rev. Lett.* **1994**, *72*, 936.

MA950605T